CHAPTER 1

Fractal Geometries

1.1 Introduction

The end of the 1970s saw the idea of *fractal geometry* spread into numerous areas of physics. Indeed, the concept of fractal geometry, introduced by B. Mandelbrot, provides a solid framework for the analysis of natural phenomena in various scientific domains. As Roger Pynn wrote in *Nature*, "If this opinion continues to spread, we won't have to wait long before the study of fractals becomes an obligatory part of the university curriculum."

The *fractal* concept brings many earlier mathematical studies within a single framework. The objects concerned were invented at the end of the 19th century by such mathematicians as Cantor, Peano, etc. The term "*fractal*" was introduced by B. Mandelbrot (fractal, i.e., that which has been infinitely divided, from the Latin "*fractus*," derived from the verb "*frangere,*" to break). It is difficult to give a precise yet general definition of a fractal object; we shall define it, following Mandelbrot, as a set which shows irregularities on all scales.

Fundamentally it is its *geometric* character which gives it such great scope; fractal geometry forms the missing complement to Euclidean geometry and crystalline symmetry.[1] As Mandelbrot has remarked, clouds are not spheres, nor mountains cones, nor islands circles and their description requires a different geometrization.

As we shall show, the idea of fractal geometry is closely linked to properties invariant under change of scale: a fractal structure is the same "*from near or from far*." The concepts of self-similarity and scale invariance appeared independently in several fields; among these, in particular, are critical phenomena and second order phase transitions.[2] We also find fractal geometries in particle trajectories, hydrodynamic lines of flux, waves, landscapes, mountains, islands and rivers, rocks, metals, and composite materials, plants, polymers, and gels, etc.

---

[1] We must, however, add here the recent discoveries about quasicrystalline symmetries.

[2] We shall not refer here to the wide and fundamental literature on critical phenomena, renormalization, etc.

Many works on the subject have been published in the last 10 years. Basic works are less numerous: besides his articles, B. Mandelbrot has published general books about his work (Mandelbrot, 1975, 1977, and 1982); the books by Barnsley (1988) and Falconer (1990) both approach the mathematical aspects of the subject. Among the books treating fractals within the domain of the physical sciences are those by Feder (1988) and Vicsek (1989) (which particularly concentrates on growth phenomena), Takayasu (1990), or Le Méhauté (1990), as well as a certain number of more specialized (Avnir, 1989; Bunde and Havlin, 1991) or introductory monographs on fractals (Sapoval, 1990). More specialized reviews will be mentioned in the appropriate chapters.

1.2 The notion of dimension

A common method of measuring a length, a surface area or a volume consists in covering them with boxes whose length, surface area or volume is taken as the unit of measurement (Fig. 1.2.1). This is the principle which lies behind the use of multiple integration in calculating these quantities.

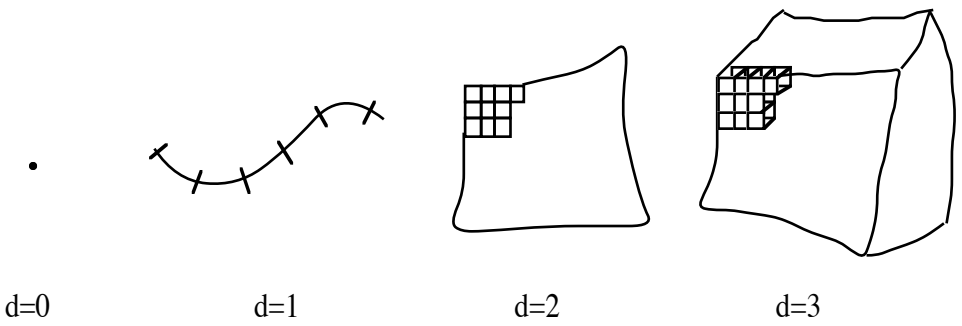

Fig. 1.2.1. Paving with lines, surfaces, or volumes.

If ε is the side (standard length) of a box and d its Euclidean dimension, the measurement obtained is

$$\mathcal{M} = N\,\varepsilon^d = N\mu,$$

where μ is the unit of measurement (length, surface area, or volume in the present case, mass in other cases). Cantor, Carathéodory, Peano, etc. showed that there exist pathological objects for which this method fails. The measurement above must then be replaced, for example, by the α-dimensional Hausdorff measure. This is what we shall now explain.

The length of the Brittany's coastline

Imagine that we would like to apply the preceding method to measure the length, between two fixed points, of a very jagged coastline such as that of

Brittany.[3] We soon notice that we are faced with a difficulty: the length $\mathcal{L}$ depends on the chosen unit of measurement ε and increases indefinitely as ε decreases (Fig. 1.2.2)!

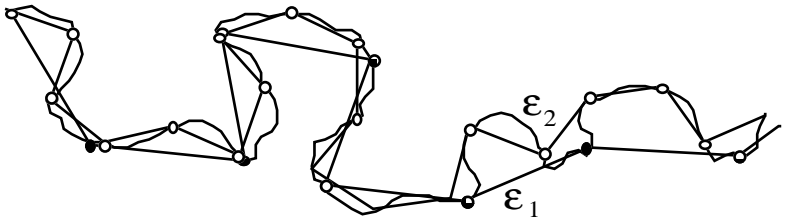

Fig. 1.2.2. Measuring the length of a coastline in relation to different units.

For a standard unit ε_1 we get a length $N_1\ \varepsilon_1$, but a smaller standard measure, ε_2, gives a new value which is larger,

$$\mathcal{L}(\varepsilon_1) = N_1\ \varepsilon_1$$
$$\mathcal{L}(\varepsilon_2) = N_2\ \varepsilon_2 \neq \mathcal{L}(\varepsilon_1)$$
$$\ldots$$

and this occurs on scales going from several tens of kilometers down to a few meters. L.F. Richardson, in 1961, studied the variations in the approximate length of various coastlines and noticed that, very generally speaking, over a

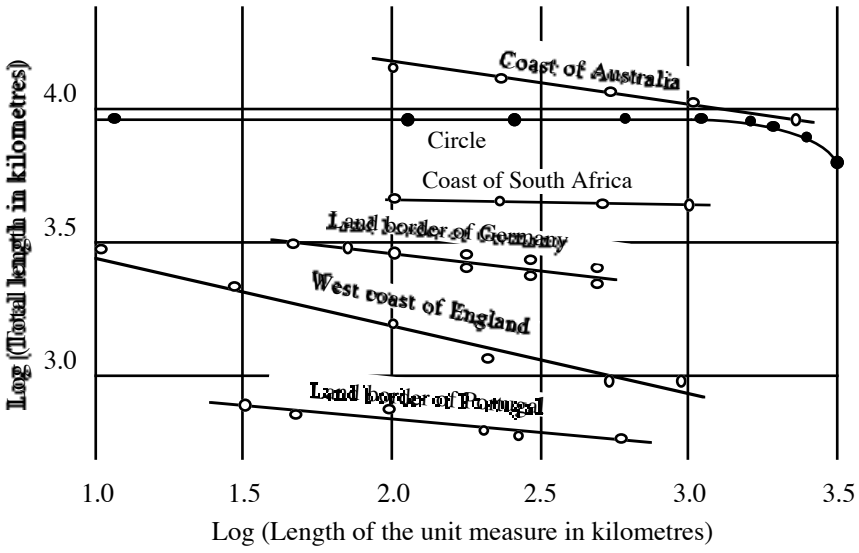

Fig. 1.2.3 Measurements of the lengths of various coastlines and land borders carried out by Richardson (1961)

[3] See the interesting preface of J. Perrin (1913) in *Atoms*, Constable (London).

large range of $\mathcal{L}(\varepsilon)$, the length follows a power law[4] in ε,

$$\mathcal{L}(\varepsilon) = N(\varepsilon)\,\varepsilon \propto \varepsilon^{-\rho}.$$

Figure 1.2.3 shows the behavior of various coastlines as functions of the unit of measurement. We can see that for a "normal" curve like the circle, the length remains constant ($\rho = 0$) when the unit of measurement becomes small enough in relation to the radius of curvature. The dimension of the circle is of course $D = 1$ (and corresponds to $\rho = 0$). The other curves display a positive exponent ρ so that their length grows indefinitely as the standard length decreases: it is impossible to give them a precise length, they are said to be nonrectifiable.[5] Moreover, these curves also prove to be nondifferentiable.

The exponent $(1+\rho)$ of $1/N(\varepsilon)$ defined above is in fact the "*fractal dimension*" as we shall see below. This method of determining the fractal size by covering the coast line with discs of radius ε is precisely the one used by Pontrjagin and Schnirelman (1932) (Mandelbrot, 1982, p. 439) to define the *covering dimension*. The idea of defining the dimension on the basis of a covering ribbon of width 2ε had already been developed by Minkowski in 1901. We shall therefore now examine these methods in greater detail.

Generally speaking, studies carried out on fractal structures rely both on those concerning nondifferentiable functions (Cantor, Poincaré, and Julia) and on those relating to the measure (dimension) of a closed set (Bouligand, Hausdorff, and Besicovitch).

1.3 Metric properties: Hausdorff dimension, topological dimension

Several definitions of fractal dimension have been proposed. These mathematical definitions are sometimes rather formal and initially not always very meaningful to the physicist. For a given fractal structure they usually give the same value for the fractal dimension, but this is not always the case. With some of these definitions, however, the calculations may prove easier or more precise than with others, or better suited to characterize a physical property.

Before giving details of the various categories of fractal structures, we shall give some mathematical definitions and various methods for calculating dimensions; for more details refer to Tricot's work (Tricot, 1988), or to Falconer's books (Falconer, 1985, 1990).

First, we remark that to define the dimension of a structure, this structure must have a notion of distance (denoted $|x-y|$) defined on it between any two of its points. This hardly poses a problem for the structures provided by nature.

---

[4] The commonly used notation '$\propto$' means 'varies as': $a \propto b$ means precisely that the ratio a/b asymptotically tends towards a nonzero constant.

[5] A part of a curve is rectifiable if its length can be determined.

We should also mention that in these definitions there is always a passage to the limit $\varepsilon^- 0$. For the actual calculation of a fractal dimension we are led to discretize (i.e., to use finite basic lengths ε): the accuracy of the calculation then depends on the relative lengths of the unit ε, and that of the system (Sec. 1.4.4).

1.3.1 The topological dimension d_T

If we are dealing with a geometric object composed of a set of points, we say that its fractal dimension is $d_T = 0$; if it is composed of line elements, $d_T = 1$, surface elements $d_T = 2$, etc.

> "Composed" means here that the object is locally homeomorphic to a point, a line, a surface. The topological dimension is invariant under invertible, continuous, but not necessarily differentiable, transformations (homeomorphisms). The dimensions which we shall be speaking of are invariant under differentiable transformations (dilations).

A fractal structure possesses a fractal dimension strictly greater than its topological dimension.

1.3.2 The Hausdorff–Besicovitch dimension, or covering dimension: dim(E)

The first approach to finding the dimension of an object, E, follows the usual method of covering the object with boxes (belonging to the space in which the object is embedded) whose measurement unit $\mu = \varepsilon^{d(E)}$, where d(E) is the Euclidean dimension of the object. When d(E) is initially unknown, one possible solution takes $\mu = \varepsilon^\alpha$ as the unit of measurement for an unknown exponent α. Let us consider, for example, a square (d = 2) of side L, and cover it with boxes of side ε. The measure is given by $\mathcal{M} = N\mu$, where N is the number of boxes, hence $N = (L/\varepsilon)^d$. Thus,

$$\mathcal{M} = N\,\varepsilon^\alpha = (L/\varepsilon)^d\,\varepsilon^\alpha = L^2\,\varepsilon^{\alpha-2}$$

If we try $\alpha = 1$, we find that $\mathcal{M} \to \infty$ when $\varepsilon \to 0$: the "length" of a square is infinite. If we try $\alpha = 3$, we find that $\mathcal{M} \to 0$ when $\varepsilon \to 0$: the "volume" of a square is zero. The surface area of a square is obtained only when $\alpha = 2$, and its dimension is the same as that of a surface $d = \alpha = 2$.

The fact that this method can be applied for any real α is very interesting as it makes possible its generalization to noninteger dimensions.

We can formalize this measure a little more. First, as the object has no specific shape, it is not possible, in general, to cover it with identical boxes of side ε. But the object E may be covered with balls V_i whose diameter (diam V_i) is less than or equal to ε. This offers more flexibility, but requires that the inferior limit of the sum of the elementary measures be taken as $\mu = (\text{diam } V_i)^\alpha$.

Therefore, we consider what is called the α–covering measure (Hausdorff, 1919; Besicovitch, 1935) defined as follows:

$$m^{\alpha}(E) = \lim_{\varepsilon \to 0} \inf\{ \sum (\text{diam } V_i)^{\alpha} : \cup V_i \supset E, \text{diam } V_i \leq \varepsilon\}, \qquad (1.3\text{-}1)$$

and we define the *Hausdorff* (or Hausdorff–Besicovitch) *dimension*: dim E by

$$\begin{aligned} \dim E &= \inf \{ \alpha : m^{\alpha}(E) = 0 \} \\ &= \sup \{ \alpha : m^{\alpha}(E) = \infty \}. \end{aligned} \qquad (1.3\text{-}2)$$

The Hausdorff dimension is the value of α for which the measure jumps from zero to infinity. For the value α = dim E, this measure may be anywhere between zero and infinity.

The function $m^{\alpha}(E)$ is monotone in the sense that if a set F is included in E, $E \supset F$, then $m^{\alpha}(E) \geq m^{\alpha}(F)$ whatever the value of α.

1.3.3 The Bouligand–Minkowski dimension

We can also define a dimension known as the Bouligand–Minkowski dimension (Bouligand, 1929; Minkowski, 1901), denoted $\Delta(E)$. Here are some methods of calculating $\Delta(E)$:

The Minkowski sausage (Fig. 1.3.1)

Let E be a fractal set embedded in a d-dimensional Euclidean space (more precisely E is a closed subset of $\mathbb{R}^d$). Now let $E(\varepsilon)$ be the set of points in $\mathbb{R}^d$ at a distance less than ε from E. $E(\varepsilon)$ now defines a Minkowski sausage: it is also called a thickening or dilation of E as in image analysis. It may be defined as the union

$$E(\varepsilon) = \bigcup_{x \in E} B_{\varepsilon}(x),$$

where $B_{\varepsilon}(x)$ is a ball of the d-dimensional Euclidean space, centered at x and of radius ε. We calculate,

$$\Delta(E) = \lim_{\varepsilon \to 0} \left(d - \frac{\log \text{Vol}_d[E(\varepsilon)]}{\log \varepsilon} \right), \qquad (1.3\text{-}3)$$

where Vol_d simply represents the volume in d dimensions (e.g., the usual length, surface area, or volume). If the limit exists, $\Delta(E)$ is, by definition, the *Bouligand–Minkowski dimension*.

Naturally, we recover from this the usual notion of dimension: let us take as an example a line segment of length L. The associated Minkowski sausage has as volume $\text{Vol}_d(E)$,

$$\begin{aligned} &\text{in } d = 2 : \quad 2\varepsilon L + \pi\varepsilon^2, \\ &\text{in } d = 3 : \quad \pi\varepsilon^2 L + (4\pi/3)\varepsilon^3, \end{aligned}$$

Fig. 1.3.1. Minkowski sausage or thickening of a curve E.

so that neglecting higher orders in ε, $\mathrm{Vol}_d(E) \propto \varepsilon^{d-1}$.

In general terms we have:

If E is a point:	$\mathrm{Vol}_d(E) \propto \varepsilon^d$,	$\Delta(E) = 0$.
If E is a rectifiable arc:	$\mathrm{Vol}_d(E) \propto \varepsilon^{d-1}$,	$\Delta(E) = 1$.
If E is a k-dimensional ball:	$\mathrm{Vol}_d(E) \propto \varepsilon^{d-k}$,	$\Delta(E) = k$.

In practice, $\Delta(E)$ is obtained as the slope of the line of least squares of the set of points given by the plane coordinates,

$$\{ \log 1/\varepsilon, \quad \log \mathrm{Vol}_d [E(\varepsilon)/\varepsilon^d] \}.$$

This method is easy to use. The edge effects (like those obtained above in measuring a segment of length L) lead to a certain inaccuracy in practice (i.e., to a curve for values of ε which are not very small).

The box-counting method (Fig. 1.3.2)

This is a very useful method for many fractal structures. Let $N(\varepsilon)$ be the number of boxes of side ε covering E:

$$\Delta(E) = \lim_{\varepsilon \to 0} \left(\frac{\log N(\varepsilon)}{-\log \varepsilon} \right) \qquad (1.3\text{-}4)$$

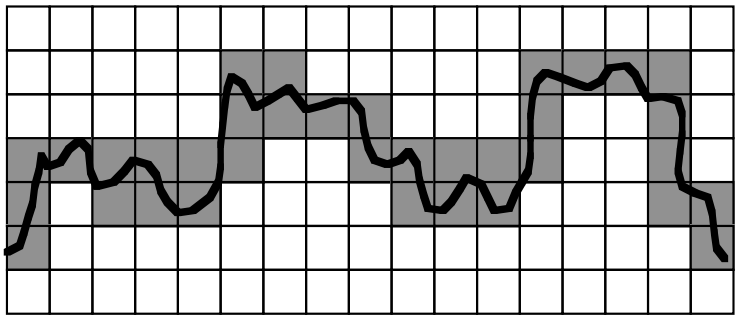

Fig.1.3.2. Measurement of the dimension of a curve by the box-counting method.

The box-counting method is commonly used, particularly for self-affine structures (see Sec. 2.2.5).

The dimension of a union of sets is equal to the largest of the dimensions of these sets: $\Delta(E \cup F) = \max \{\Delta(E), \Delta(F)\}$.

The limit $\Delta(E)$ may depend on the choice of paving. If there are two different limits Sup and Inf, the Sup limit should be taken.

The disjointed balls method (Fig 1.3.3)

Let $N(\varepsilon)$ be the *maximum* number of disjoint balls of radius ε centered on the set E: then

$$\Delta(E) = \lim_{\varepsilon \to 0} \log N(\varepsilon) / |\log \varepsilon| \, . \qquad (1.3\text{-}5)$$

This method is rarely used in practice.

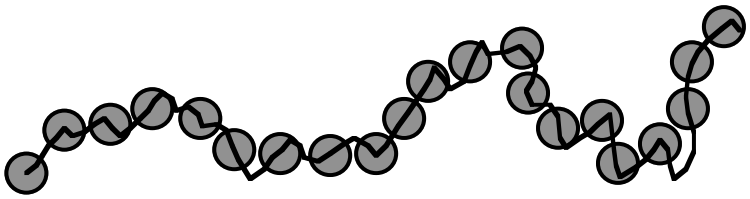

Fig.1.3.3. Measuring the dimension of a curve by the disjointed balls method.

The dividers' method (Richardson, 1960)

This is the method we described earlier (Fig. 1.2.2).

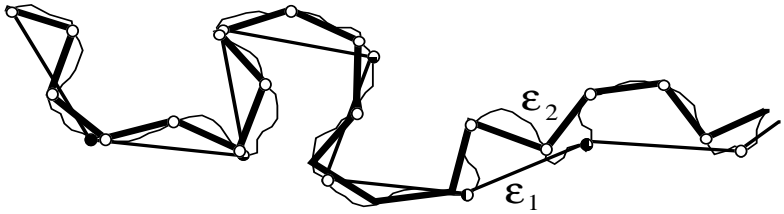

Let $N(\varepsilon)$ be the number of steps of length ε needed to travel along E:

$$\Delta(E) = \lim_{\varepsilon \to 0} \log N(\varepsilon) / |\log \varepsilon| \qquad (1.3\text{-}6)$$

Notice that all the methods give the same fractal dimension, $\Delta(E)$, when it exists (see Falconer, 1990), because we are in a finite dimensional Euclidean space. This is no longer true in an infinite dimensional space, (function space, etc.).

1.3.4 The packing dimension [or Tricot dimension: Dim (E)]

Unlike the Hausdorff–Besicovitch dimension, which is found using the α-dimensional Hausdorff measure, the box-counting dimension $\Delta(E)$ is not defined in terms of measure. This may lead to difficulties in certain theoretical developments. This problem may be overcome by defining the packing dimension, following similar ideas to those of the α-dimensional Hausdorff measure (Falconer, 1990). Let $\{V_i\}$ be a collection of disjoint balls, and

$$\mathcal{P}_o{}^{\alpha}(E) = \lim_{\varepsilon \to 0} \sup\{ \sum(\text{diam } V_i)^{\alpha}, \text{diam } V_i \le \varepsilon\}.$$

As this expression is not always a measure we must consider

$$\mathcal{P}^{\alpha}(E) = \inf\{ \mathcal{P}_o^{\alpha}(E_i) : \bigcup_{i=1}^{\infty} E_i \supset E\} \ .$$

The packing dimension is defined by the following limit:

$$\text{Dim } E = \sup\{\alpha : \mathcal{P}^{\alpha}(E) = \infty \} = \inf \{\alpha : \mathcal{P}^{\alpha}(E) = 0 \}, \qquad (1.3\text{-}7a)$$

alternatively, according to the previous definitions:

$$\text{Dim } E = \inf\{\sup \Delta(E_i) : \cup E_i \supset E\}. \qquad (1.3\text{-}7b)$$

The following inequalities between the various dimensions defined above are always true:

$$\begin{aligned} \dim E \le \text{Dim } E &\le \Delta(E) \\ \dim E + \dim F &\le \dim E \otimes F \\ &\le \dim E + \text{Dim } F \\ &\le \text{Dim } E \otimes F \le \text{Dim } E + \text{Dim } F. \end{aligned}$$

Notice that for multifractals box-counting dimensions are in practice rather Tricot dimensions.

Other methods of calculation have been proposed by Tricot (Tricot, 1982) which could prove attractive in certain situations. Without entering into the details, we should also mention the *method of structural elements*, the *method of variations* and the *method of intersections*.

Theorem: If there exists a real D and a finite positive measure μ such that for all $x \in E$, ($B_r(x)$ being the ball of radius r centered at x),

$$\log \mu[B_r(x)]/\log r \to D, \text{ then}$$

$$D = \dim E. \qquad (1.3\text{-}8)$$

D is also called the *mass dimension*. If the convergence is uniform on E, then

$$D = \dim(E) = \Delta(E). \qquad (1.3\text{-}9)$$

This theorem does not always apply: dim E = 0 for a denumerable set, while for the Bouligand–Minkowski dimension $\Delta(E) \neq 0$.

In practice, Mandelbrot has popularized the Hausdorff–Besicovitch dimension or mass dimension (as the measure is very often a mass), dim E, which turns out to be one of the simpler and more understandable dimensions (although not always the most appropriate) for the majority of problems in physics *when the above theorem applies*.

So we now have the following relation giving the mass inside a ball of radius r,

$$\boxed{\mathcal{M} = \mu(B_r(x)) \propto r^D}, \qquad (1.3\text{-}10)$$

where the center x of the ball B is inside the fractal structure E.

We shall of course take the physicist's point of view and not burden ourselves, at first, with too much mathematical rigor. The *fractal dimension will in general be denoted* D and, in the cases considered, we shall suppose that, unless specified otherwise, the existence theorem applies and therefore that the fractal dimension is the same for all the methods described above.

Units of measure

The above relation can often be written in the form of a dimensionless equation, by introducing the unit of length ε_u and volume $(\varepsilon_u)^d$ or mass $\rho_u = (\varepsilon_u)^d \rho$ (by assuming a uniform density ρ over the support):

$$\frac{\mathcal{V}}{(\varepsilon_u)^d} \quad \text{or} \quad \frac{\mathcal{M}}{\rho_u} \propto \left(\frac{r}{\varepsilon_u}\right)^D .$$

Examples of this for the Koch curve and the Sierpinski gasket will be given later in Sec. 1.4.1. In this case the unit of volume is that of a space with dimension equal to the topological dimension of the geometric objects making up the set (see Sec. 1.3.1).

From a strictly mathematical point of view the term "dimension" should be reserved for sets. For measures, we can think of the set covered by a uniform measure. However, we can define the dimension of a measure by

$$\dim(\mu) = \inf \{ \dim(A), \mu(A^c)=0 \},$$

A being a measurable set and A^c its complement. This dimension is often strictly less than the dimension of the support. This happens with the information dimension described in Sec. 1.6.2.

For objects with a different scaling factor in different spatial directions, the box-counting dimension differs from the Hausdorff dimension (see Fig. 2.2.8).

Having defined the necessary tools for studying fractal structures, it is now time to get to the heart of the matter by giving the first concrete examples of fractals.

1.4 Examples of fractals

1.4.1 Deterministic fractals

Some fractal structures are constructed simply by using an iterative process consisting of an initiator (initial state) and a generator (iterative operation).

The triadic Von Koch curve (1904)

Each segment of length ε is replaced by a broken line (*generator*), composed of four segments of length ε/3, according to the following recurrence relation:

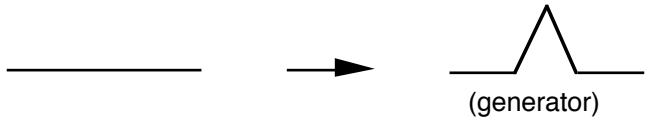

At iteration zero, we have an *initiator* which is a segment in the case of the triadic Koch curve, or an equilateral triangle in the case of the Koch island. If the initiator is a segment of horizontal length L, at the first iteration (the curve coincides with the generator) the base segments will have length $\varepsilon_1 = L/3$;

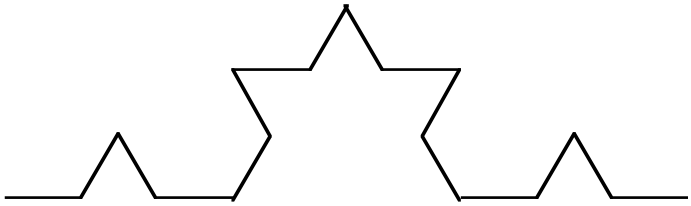

at the second iteration they will have length $\varepsilon_2 = L/9$ as each segment is again replaced by the generator, then $\varepsilon_3 = L/3^3$ at the third iteration

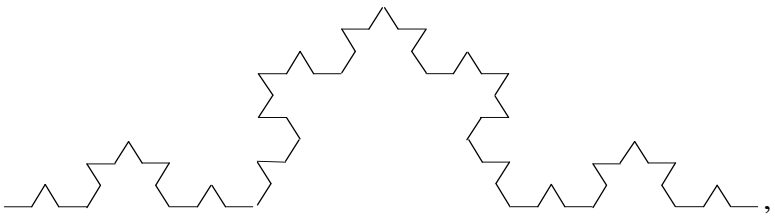

and so on. The relations giving the length $\mathcal{L}$ of the curve are thus

$$\begin{aligned} \varepsilon_1 = L/3 \;&\rightarrow\; \mathcal{L}_1 = 4\,\varepsilon_1 \\ \varepsilon_2 = L/9 \;&\rightarrow\; \mathcal{L}_2 = 16\,\varepsilon_2 \\ &\cdots \\ \varepsilon_n = L/3^n \;&\rightarrow\; \mathcal{L}_n = 4^n\,\varepsilon_n \end{aligned}$$

by eliminating n from the two equations in the last line, the length $\mathcal{L}_n$ may be written as a function of the measurement unit ε_n

$$\mathcal{L}_n = L^D\,(\varepsilon_n)^{1-D} \quad \text{where } D = \log 4 / \log 3 = 1.2618\ldots$$

For a *fixed unit length* ε_n, $\mathcal{L}_n$ grows as the Dth power of the size L of the curve. Notice that here again we meet the exponent $\rho = D-1$ of ε_n, which we first met in Sec. 1.2 (Richardson's law) and which shows the divergence of $\mathcal{L}_n$ as $\varepsilon_n \rightarrow 0$.

At a given iteration, the curve obtained is not strictly a fractal but according to Mandelbrot's term a "prefractal". A fractal is a mathematical object obtained in the limit of a series of prefractals as the number of iterations n tends to infinity. In everyday language, prefractals are often both loosely called "fractals".

The previous expression is the first example given of a scaling law which may be written

$$\mathcal{L}_n / \varepsilon_n = f(L/\varepsilon_n) = (L/\varepsilon_n)^D \quad . \tag{1.4-1}$$

A scaling law is a relation between different *dimensionless* quantities describing the system, (the relation here is a simple power law). Such a law is generally possible only when there is a single independent unit of length in the object (here ε_n).

A structure associated with the Koch curve is obtained by choosing an equilateral triangle as initiator. The structure generated in this way is the well-known *Koch island* (see Fig. 1.4.1).

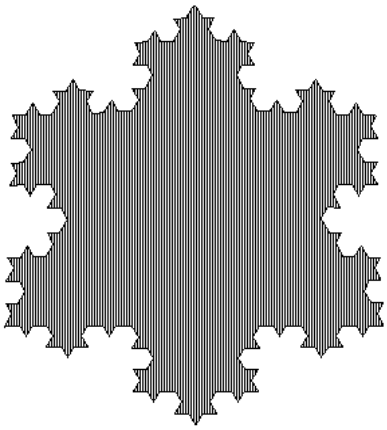

Fig. 1.4.1. Koch island after only three iterations. Its coastline is fractal, but the island itself has dimension 2 (it is said to be a surface fractal).

Simply by varying the generator, the Koch curve may be generalized to give curves with fractal dimension $1 \le D \le 2$. A straightforward example is provided by the modified Koch curve whose generator is

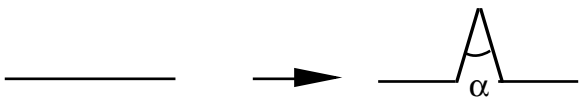

and whose fractal dimension is $D = \log 4 / \log [2 + 2 \sin(\alpha/2)]$. Notice that in the limit $\alpha = 0$ we have $D = 2$, that is to say a curve which fills a triangle. It is not exactly a curve as it has an infinite number of multiple points. But the construction can be slightly modified to eliminate them. The dimension $D = 2$

(= log 9/log 3) is also obtained for the *Peano curve* (Fig. 1.4.2) (which is dense in a square) whose generator is formed from 9 segments with a change by a factor 3 in the linear dimension, i.e.,

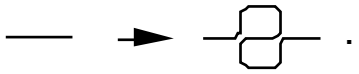

This gives after the first three iterations,

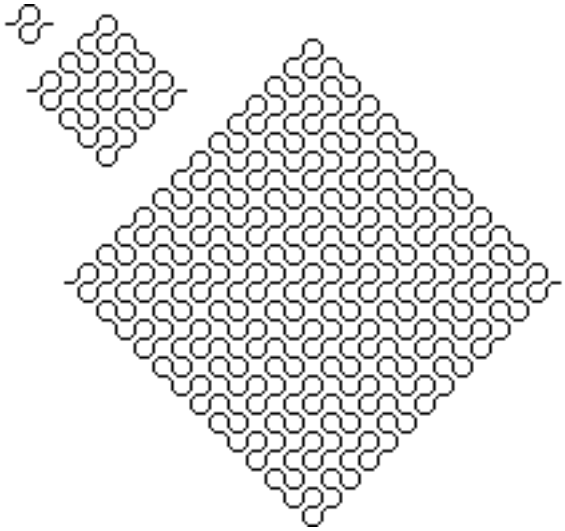

Fig. 1.4.2. First three iterations of the Peano curve (for graphical reasons the scale is simultaneously dilated at each iteration by a factor of 3). The Peano curve is dense in the plane and its fractal dimension is 2.

This construction has also been modified (rounding the angles) to eliminate double points.

The von Koch and Peano curves are as their name indicates: curves, that is, their *topological dimension* is

$$d_T = 1.$$

Practical determination of the fractal dimension using the mass-radius relation

As mentioned earlier, a method which we shall be using frequently to determine fractal dimensions[6] consists in calculating the mass of the structure within a ball of dimension d centered on the fractal. If the embedding space is d-dimensional, and of radius R, then

$$\mathcal{M} \propto R^D.$$

The measure here is generally a mass, but it could equally well be a "surface area" or any other scalar quantity attached to the support (Fig. 1.4.3).

[6] The box-counting method will also be frequently used.

In the case of the Koch curve, we could check to see that D = log 4/log 3, as is the case for the different methods shown above. Notice that if the ε_n are not chosen in the sequence $\varepsilon_n = L/3^n$, the calculations prove much more complicated, but the limit as $\varepsilon \to 0$ still exists and gives D.

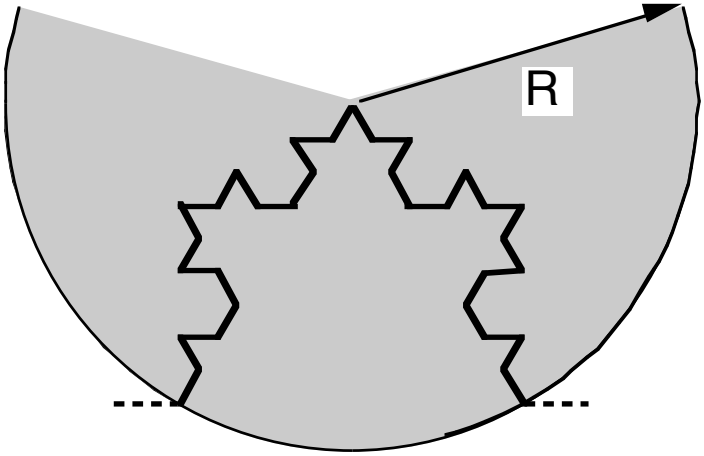

Fig. 1.4.3. Measuring the fractal dimension of a Koch curve using the relationship bet-ween mass and radius. If each segment represents a unit of "fractal surface area" (1 cm^D, say), the "surface area" above is equal to 2 cm^D when R = 1 cm, 8 cm^D when R = 3 cm.

In very general terms $\mathcal{M}$ has the form,

$$\mathcal{M} = A(R)\ R^D$$

where $A(R) = A_0 + A_1\ R^{-\Omega} + \ldots$ tends to a constant A_0 as $R \to \infty$. When the coefficients $A_1, \ldots$ are nonzero (which is not the case for the examples in this chapter), A(R) is called the scaling law correction.

Direct determination of the fractal dimension and the multiscale case

The fractal dimension D may be found directly from a single iteration *if the limit structure is known to be a fractal*. If a fractal structure of size L with mass $\mathcal{M}(L) = A(L)\ L^D$ gives after iteration k elements of size L/h, we then have an implicit relation in D:

$$\mathcal{M}(L) = k\,\mathcal{M}(L/h), \text{ hence } A(L)\ L^D = k\ A(L/h)\ (L/h)^D.$$

D is thus determined asymptotically ($L \to \infty$) by noticing that

$$A(L/h) / A(L) \to 1 \text{ as } L \to \infty. \text{ Hence } k\ (1/h)^D = 1.$$

For example, the Koch curve corresponds to k = 4 and h = 3. Moreover, A(L) is independent of L here.

Later on we shall meet *multiscale fractals*, giving at each iteration k_i elements of size L/h_i (i = 1,…, n). Thus

$$\mathcal{M}(L) = k_1 \mathcal{M}(L/h_1) + k_2 \mathcal{M}(L/h_2) + \ldots + k_n \mathcal{M}(L/h_n),$$

which means that the mass of the object of linear size L is the sum of k_i masses of similar objects of size L/h_i. Thus,

$$k_1 (1/h_1)^D + k_2 (1/h_2)^D \ldots + k_n (1/h_n)^D = 1, \qquad (1.4\text{-}2)$$

which determines D.

Cantor sets

These are another example of objects which had been much studied before the idea of fractals was introduced. The following Cantor set is obtained by iteratively deleting the central third of each segment:

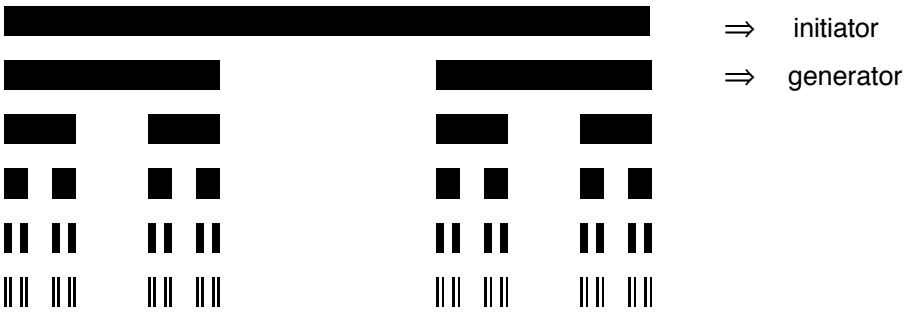

Fig. 1.4.4. Construction of the first five iterations of a Cantor set. In order to have a clearer representation and to introduce the link between measure and set, the segments have been chosen as bars of fixed width (Cantor bars), consequently representing a uniform density distributed over the support set (uniform measure, see also Sec.1.6.3). In this way the fractal dimension and the mass dimension are identified.

Five iterations are shown in Fig. 1.4.4.

The fractal dimension of this set is

$$D = \log 2 / \log 3 = 0.6309...$$

For Cantor sets we have $0 < D < 1$: it is said to be a "dust." As it is composed only of points, its *topological dimension* is $d_T = 0$.

To demonstrate the fact that the fractal dimension by itself does not uniquely characterize the object, we now construct a second Cantor set with the same fractal dimension but a different spatial structure (Fig. 1.4.5): at each iteration, each element is divided into four segments of length 1/9, which is equivalent to uniformly spacing the elements of the second iteration of the previous set. In fact these two sets differ by their lacunarity (cf. Sec. 1.5.3), that is, by the distribution of their empty regions.

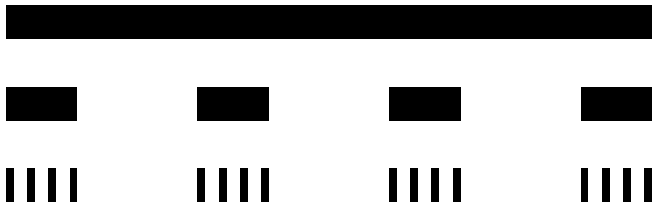

Fig. 1.4.5. Construction of the first two iterations of a different Cantor set having the same fractal dimension.

Mandelbrot–Given curve

Iterative deterministic processes have shown themselves to be of great value in the study of the more complex fractal structures met with in nature, since their iterative character often enables an exact calculation to be made. The Mandelbrot-Given curve (Mandelbrot and Given, 1984) is an instructive example of this as it simulates the current conducting cluster of a network of resistors close to their conductivity threshold (a network of resistors so many of which are cut that the network barely conducts). It is equally useful for understanding multifractal structures (see Fig. 1.4.6). We shall take this up again in Sec 5.2.2 (hierarchical models) as it is a reasonable model for the "backbone" of the infinite percolation cluster (Fig. 3.1.8).

The generator and first two iterations are as follows:

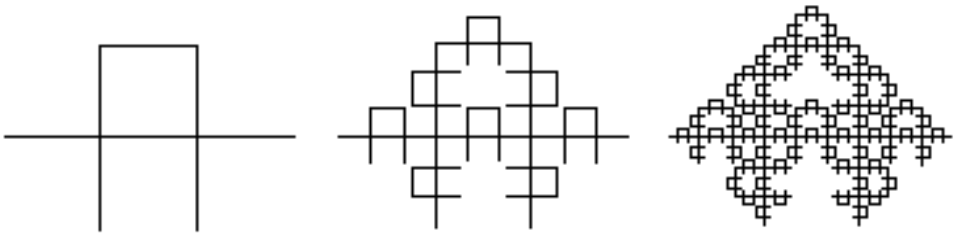

Fig. 1.4.6. Construction of the first three iterations of a Mandelbrot–Given set. This fractal has a structure reminiscent of the percolation cluster which plays an important role in the description of disordered media (Sec. 3.1).

The vertical segments of the generator are slightly shortened to avoid double points. The fractal dimension (neglecting the contraction of the vertical segments) is $D = \log 8/ \log 3 \cong 1.89\ldots$.

"Gaskets" and "Carpets"

These structures are frequently used to carry out exact, analytic calculations of various physical properties (conductance, vibrations, etc.).

Sierpinski gasket

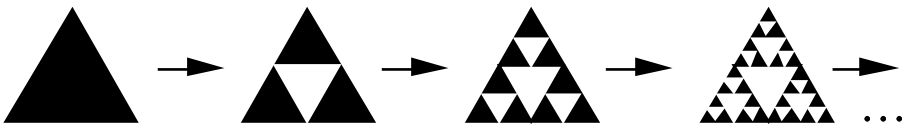

Fig. 1.4.7. Iteration of the Sierpinski gasket composed of full triangles (the object is made up only of those parts left coloured black).

The scaling factor of the iteration is 2, while the mass ratio is 3 (see Fig. 1.4.7). The corresponding fractal dimension is thus

$$D = \log 3/\log 2 = 1.585\ldots$$

The Sierpinski gasket generated by the edges only is also often used (see Fig. 1.4.8). It clearly has the same fractal dimension $D = \log 3/\log 2 = 1.585\ldots$

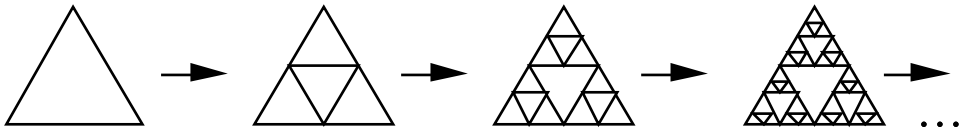

Fig. 1.4.8. Iteration of the Sierpinski gasket composed of sides of triangles.

The two structures can be shown to "converge" asymptotically towards one other, in the sense of the Hausdorff distance (see, e.g., Barnsley, 1988).

Sierpinski carpet

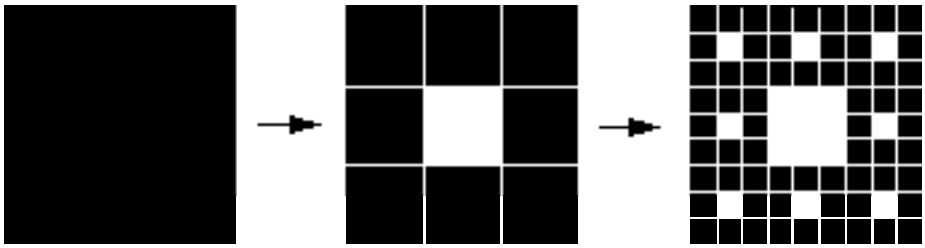

Fig. 1.4.9. Iteration of a Sierpinski carpet.

The scaling factor is 3 and the mass ratio (black squares) is 8 (see Fig. 1.4.9). Hence,

$$D = \log 8/\log 3 = 1.8928\ldots$$

Other examples

Examples of deterministic fractal structures constructed on the basis of the Sierpinski gasket and carpet can be produced endlessly. These geometries can

prove very important for modelling certain transport problems in porous objects or fractal electrodes. Here are a couple of three-dimensional examples, the 3d gasket and the so-called Menger sponge (Fig. 1.4.10).

3d gasket (Mandelbrot) D = log 4/log 2 = 2

Menger sponge D = log 20/log 3 ≅ 2.73

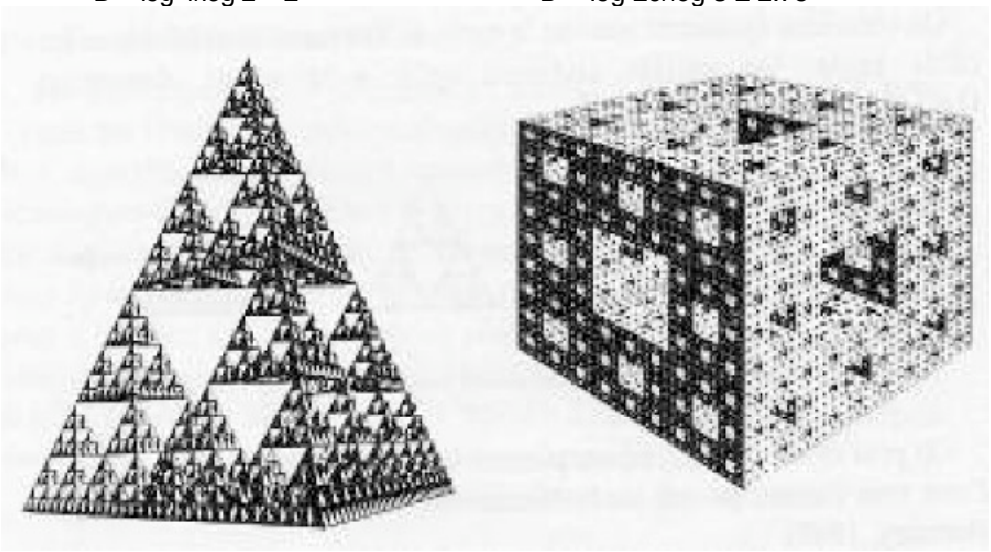

Fig. 1.4.10. Three-dimensional Sierpinski gasket composed of full tetrahedra (above left); Menger sponge (above right). (Taken from Mandelbrot, 1982.)

This again illustrates the fact that fractal dimension alone does not characterize the object: the fractal dimension of the three-dimensional gasket is equal to two, as is that of the Peano curve.

Nonuniform fractals

Another possible type of fractal structure relies on the simultaneous use of several dilation scales. Here is an example of such a structure, obtained by deterministic iteration using factors 1/4 and 1/2 (Fig. 1.4.11). This structure is clearly fractal and its dimension D is determined by one iteration, as before, (from Eq. 1.4.2):

$$4\,(L/4)^D + (L/2)^D = L^D$$

$$\text{hence} \quad D = \frac{\log(1+\sqrt{17})}{\log 2} - 1 \quad .$$

In reality, its support distribution is more complex than the fractals described above: in fact it is multifractal. Multifractal measures will be studied in greater detail in Sec. 1.6.

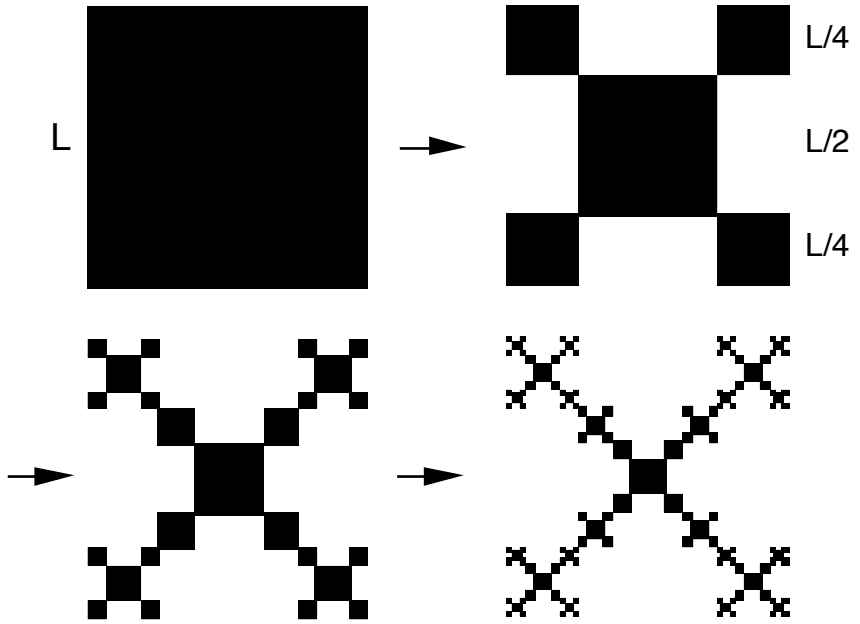

Fig. 1.4.11. Construction of a nonuniform deterministic fractal: here with two scales of contraction.

1.4.2 Random fractals

Up to now only examples of deterministic (also called "exact") fractals have been given, but random structures can easily be built. In these structures the recurrence defining the hierarchy is governed by one or more probabilistic laws which fix the choice of which generator to apply at each iteration.

Homogeneous fractals

A random fractal is homogeneous when the structure's volume (or mass) is distributed uniformly at each hierarchical level, that is, the different generators used to construct the fractal keep the same mass ratio from one level to the next.

So, from the recurrence:

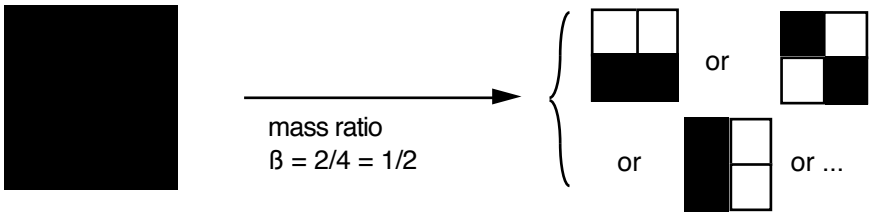

Fig. 1.4.12-a. Random fractal generator.

the following random fractal may be constructed:

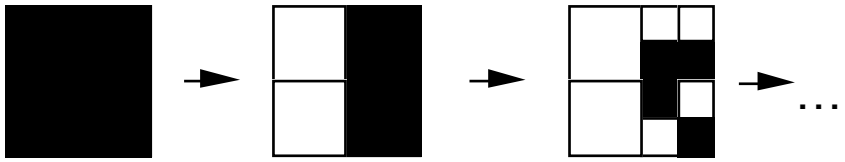

Fig. 1.4.12-b. Random fractal generated by the previous generator.

The corresponding fractal dimension is

$$D = d + \log \beta / \log 2 = 1.$$

Finding D from a single iteration, we have $2^d\beta$ new elements, each of size 1/2 at each iteration, thus $2^d\beta\,(1/2)^D = 1$.

Heterogeneous fractals

The mass ratio ß may itself vary: a fractal constructed in this way is said to be heterogeneous (Figs. 1.4.13a and 1.4.13b). This type of fractal can be used as a basis for modeling turbulence (see Sec. 2.3).

Starting with a recurrence relation, with a given distribution of ß,

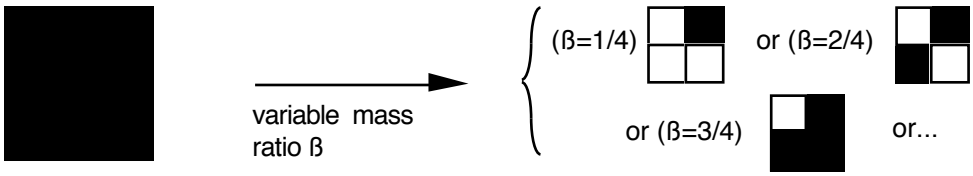

Fig. 1.4.13-a. Generator of a heterogeneous random fractal.

it is possible to build up heterogeneous fractal structures:

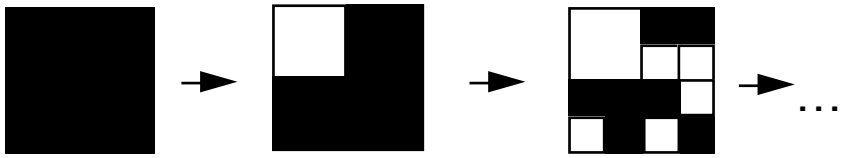

Fig. 1.4.13-b. Heterogeneous random fractal generated by the previous fractal.

whose dimension is given by $\langle \mathcal{M}(L) \rangle \propto L^D$. Hence,

$$D = d + \log \langle ß \rangle / \log 2$$

Random fractals are, with some notable exceptions, almost the only ones found in nature; their fractal properties (scale invariance, see Sec. 1.4.3) bear on the statistical averages associated with the fractal structure.

Example: Fig 1.4.14 below shows a distribution of disks ,the positions of whose centers follow a Poisson distribution, and whose radii are randomly distributed according to a probability density, $P(R>r) = Q\ r^{-\alpha}$; the larger the value of α, the higher is the frequency of smaller disks, and the further the fractal dimension of the black background is from 2. Such a distribution of disks could belong to lunar craters seen from above (projection) or holes in a piece of Emmenthal cheese! We shall be returning to this model later.

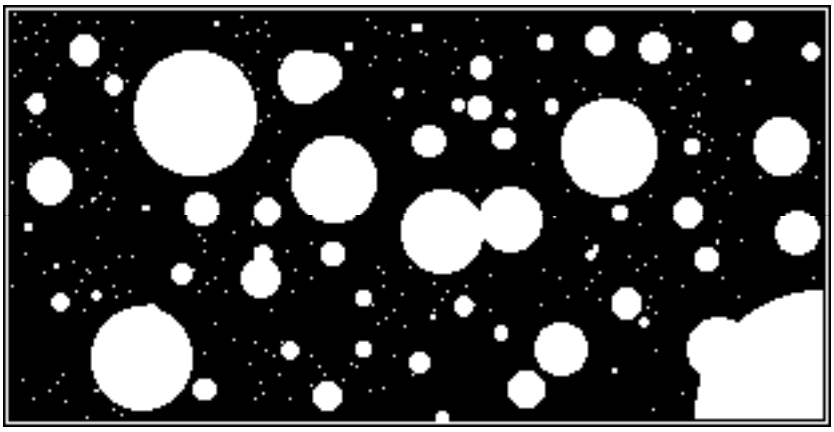

Fig. 1.4.14 Random fractal of discs whose sizes are distributed according to a power law.

In a similar way any number of fractal structures may be thought up. Examples are given in Mandelbrot (1982).

Let us now return to the basic properties of the structures we have just constructed.

1.4.3 Scale invariance

Scale invariance is also called *invariance under internal similarity* or sometimes *dilation invariance*. It is a feature which allows one to detect a fractal structure simply by looking at it: the object appears similar to itself "from near as from far," that is, whatever the scale. Naturally the eye is inadequate and a more refined analysis is required. In previous examples this invariance came from the fact that an iterative structure is such that its mass obeys a homothetic relation of the form[7] (L large)

$$\mathcal{M}(bL) = \lambda\mathcal{M}(L),$$

so that by dilating the linear dimensions of a volume by a factor b, the mass of the matter contained in this volume will be multiplied by a factor λ. For

[7] The unit of measure must be conserved in the dilation; to avoid difficulties due to a characteristic minimum size in the physical system considered (an aggregate of particles for example), we take this size to be the unit.

ordinary surfaces or volumes $\lambda = b^d$, where d is the dimension of the object. This relation generalizes to all self-similar fractals. For the Koch curve, for example,

$$\mathcal{M}(3L) = 4\mathcal{M}(L) = 3^D\mathcal{M}(L),$$

and in the general case,

$$\boxed{\mathcal{M}(bL) = b^D\,\mathcal{M}(L)}\,. \qquad (1.4\text{-}3)$$

This is a very direct method of calculating D, which is thus also *the similarity dimension*, (see also the remark p. 14).

The scale invariance relation $\mathcal{M}(bL) = b^D\,\mathcal{M}(L)$ is equivalent to the mass/radius relation $\mathcal{M}(L) = A_0L^D$. To see this, choose $b = 1/L$ in the scaling law, giving $\mathcal{M}(L) = \mathcal{M}(1)\,L^D$.

We shall see that internal similarity is present in many exact or random fractals (see below), which are not generated by iteration.

Generally speaking:

Translational invariance $\rightarrow$ periodic networks
Dilation invariance $\rightarrow$ self-similar fractals

In practice scale invariance only works for a limited range of distances r:

$$a << r << \Lambda.$$

Λ is the macroscopic limit due to the size of the sample, correlation length, effects of gradients, etc. and a is the microscopic limit due to the lattice distance, molecular sizes, etc. When we come to discuss macroscopic structures in chapter 2 (and microscopic structures in chapter 3), we mean to say that the scales of a and Λ are macroscopic (or microscopic, respectively). Moreover, if there are corrections to the scaling law [A(r) not constant], scale invariance will only be found asymptotically (for very large r).

1.4.4 Ambiguities in practical measurements

In practice, in other words, for physical objects, we find problems in applying the methods we have just described. This is partly because, as we mentioned in the last paragraph, there is both a minimum characteristic size below which the fractal description ceases to be valid (for example, aggregates composed of small particles) and also an upper size limit for the object under consideration. But it is also because a physical phenomenon, dependent on some (dominant) parameter, only generates fractal structures on all scales for a critical value of this parameter. This value is often difficult to attain, so scaling law corrections are generally required (see remark p. 14).

The fractal dimension is obtained from the slope of the linear regression of the points with coordinates, {log 1/r, log N(r)}, with r going from the minimum characteristic size to the size of the object.

The method employed to determine the dimension (discussed by Tricot, 1982), the limited extent of a fractal dynamic (object only fractal over a scale spanning less than two orders of magnitude), and the presence of scaling law corrections, all contribute to making this method based on log-log regression sometimes imprecise. Such a representation tends to straighten any curves. The presence of slight curvature is a sign that the asymptotic régime has not been reached. Furthermore, as a point of inflexion may be taken for linear behavior, it is not always obvious, without reliable theoretical support, what is happening in this case. A good theoretical model or a dynamic that extends over a sufficiently wide range of scales is therefore indispensable. A discussion about real and apparent power laws may be found in T. A. Witten, Les Houches, 1985 (Boccara and Daoud, 1985).

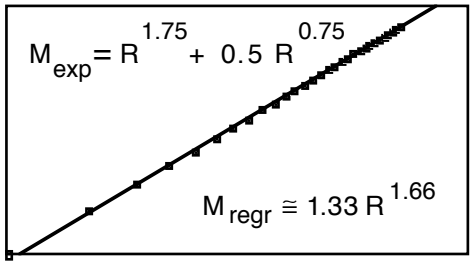

Fig. 1.4.15. Very simple example of imprecision in estimating the exponent (M_{regr}) due to corrections in the scaling law (M_{exp}). The value is found to be 1.66 instead of 1.75, in spite of the seemingly linear nature of the graph.

1.5 Connectivity properties

A fractal is insufficiently characterized by its fractal dimension D, alone. Exponents appear throughout this book with the intension of specifying the behavior of various physical quantities.

Geometrically it is interesting to consider quantities such as the *spreading*, the *ramification*, or the *lacunarity dimensions*, which characterise the properties of connectivity and of the distribution of matter within a fractal.

1.5.1 Spreading dimension, dimension of connectivity

Let us consider a fractal composed of squares lying next to each other (Fig 1.5.1). The white squares are permitted sites, the black squares are forbidden. By counting the number $S(\ell)$ of permitted sites accessible from a given permitted site in ℓ or less steps, where a step consists of passing to a bordering permitted site, generally, a mass–(distance in steps) relation of the form,

$$S(\ell) \propto \ell^{d_e} \tag{1.5-1}$$

is obtained. ℓ is called the *chemical distance* or *distance of connectivity* and d_e the *spreading dimension*. This dimension depends solely on the connections between the elements of the fractal structure (and not on the metric of the space in which it is embedded): it is an *intrinsic connectivity property* of the fractal. The dimension d_s is linked to the *tortuosity*: the higher the tortuosity, the more the convolutions of the object make us use detours to get from one point to another situated at a fixed distance "as the crow flies." We have the inequality $d_e \leq D$. The equality, $d_e = D$, is attained when the fractal metric corresponds to its natural metric, that is, when the Euclidean dimensions (as the crow flies) are equal or proportional to the distances obtained by staying inside the fractal (on average). This is the case for Sierpinski gaskets.

Because of the statistical invariance of the structure under any dilation, we would expect the mean quadratic Euclidean distance $R(\ell)^2$ between two sites separated by a "chemical distance" ℓ to be such that

$$\boxed{R(\ell)^2 \propto \ell^{2/d_{min}}}. \tag{1.5-2}$$

d_{min} is called the chemical dimension or the dimension of connectivity. It is the fractal dimension of the shortest path (the measure being the distance in steps): we then have a (distance in steps)–radius relation given by $\ell \propto R^{d_{min}}$. Since $S(\ell) \propto R(\ell)^D$ we have

$$\boxed{d_e = \frac{D}{d_{min}}} \tag{1.5-3}$$

This only agrees with our previous statement that $d_e = D$, if $d_{min} = 1$, that is, $R \propto \ell$.

The figures represent the chemical distance ℓ = 1, 2, 3,... from an origin 0.The forbidden regions are in black. The shaded areas correspond to different clusters inaccessible from 0. R is the square root of the mean square distance between two points, ℓ apart .

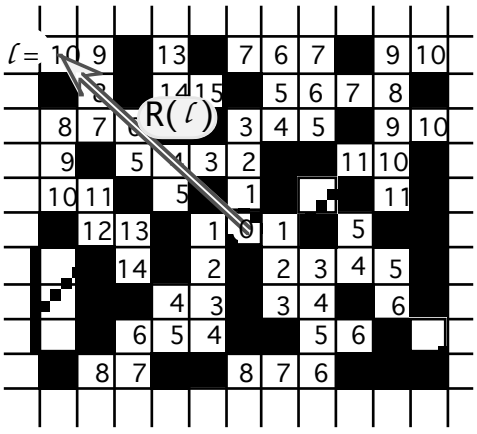

Fig. 1.5.1. Representation on a square network of accessible sites, chemical distance ℓ, and visited sites $S(\ell)$. For example, $S(3) = 11 = 3_{(1)} + 3_{(2)} + 5_{(3)}$.

1.5.2 The ramification $\mathcal{R}$

$\mathcal{R}$ is the *smallest* number of links which must be cut to *disconnect a macroscopic part* of the object. Links should be understood as paths leading from one point of the structure to another.

Thus, for the Sierpinski gasket $\mathcal{R}$ is finite, while for the carpet $\mathcal{R}$ is infinite. Ramification plays an important role in the conduction and mechanical properties of fractals. The condition that $\mathcal{R}$ be finite is, moreover, a necessary condition for *exact* relations of the renormalization group in real space. This will be proven for the example of a Sierpinski gasket, where its vibration modes are calculated in Sec. 5.1.1 and its conductance in Sec. 5.2.1.

1.5.3 The lacunarity $\mathcal{L}$

This indicates, in some sense, how far an object is from being translationally invariant, by measuring the presence of sizeable holes in a fractal structure E.

We have seen that it is always possible to write $\mathcal{M}(R)=A(R)\ R^D$, the sole condition on A being that $\log A/\log R \to 0$. The distribution of holes or lacunae is consequently related to the fluctuations around the law in R^D. The lacunarity $\mathcal{L}$ is therefore defined by

$$\mathcal{L} = \text{variance (A)},$$

that is to say, the lacunarity may be calculated from the mean over E (Fig. 1.5.2),

$$\boxed{\mathcal{L}(R) = \left(\langle \mathcal{M}(R)^2 \rangle - \langle \mathcal{M}(R) \rangle^2 \right)^{1/2} / \langle \mathcal{M}(R) \rangle} \qquad (1.5\text{-}4)$$

For an object such as the Cantor set, defined on p. 15, the lacunarity is periodic (in log R), as A(R) = A(bR), b = 1/3 and 1/4 for the first and second

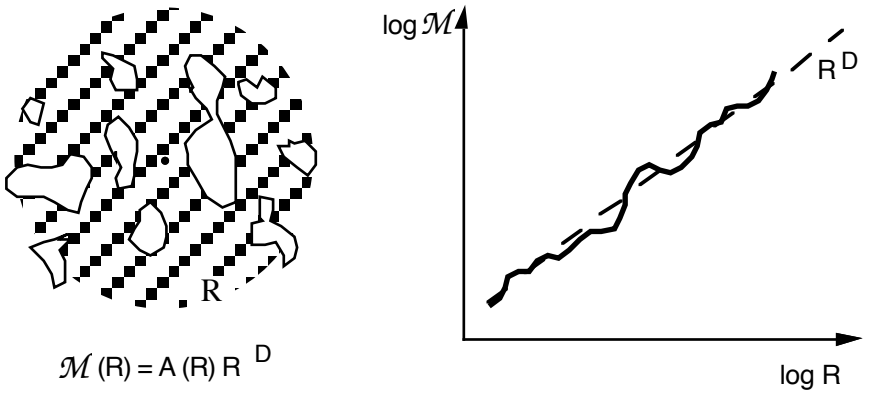

Fig. 1.5.2. Effect of lacunarity on the mass relation as a function of the radius. $\mathcal{M}(R)$ fluctuates around the power law in R^D.

examples, respectively. This is also true for deterministic fractals obtained by

iterating a generator. The lacunarity becomes aperiodic for random fractals (Gefen et al., 1983).

1.6 Multifractal measures

Knowledge of the fractal dimension of a set (as we have seen), is insufficient to characterize its geometry, and, all the more so, any physical phenomenon occurring on this set. Thus, in a random network of fusible links, the links which melt are those through the current exceeds a certain threshold. Their distribution is supported by a set whose fractal dimension generally differs from that of the whole. Likewise, in a growth phenomenon, such as diffusion limited aggregation, (the DLA model is described in Sec. 4.2), the growth sites do not all have the same weight; some of them grow much more quickly than others. Therefore, to understand many physical phenomena, involving fractal supports, the (singular) distribution of measures associated with each point of the support must be characterized. These measures, scalar quantities, may correspond to concentrations, currents, electrical or chemical potentials, probabilities of reaching each point of the support, pressures, dissipations, etc.

Intuitive approach to multifractality

Let us take as an example the distribution of diamonds over the surface of the earth. We shall suppose that the statistics governing this distribution has certain similarities with the one in Fig. 1.4.14 (a little too optimistic !): that is, we suppose that the distribution of diamonds is fractal, that it is not homogeneous, and that there exist very few regions where large stones occur: the majority of places on the earth's surface containing only traces of diamonds. The information we can draw from knowing the fractal dimension is global: if it is close to two, diamonds are spread almost uniformly throughout the world, if it is close to zero, there are a few privileged places where all of the diamonds are concentrated. In the first situation we soon find something, but the yield is very low; in the second case we must search for a long time but then we will be well paid for our efforts. We quickly realize that the information provided by the fractal dimension is inadequate. There is a *measure attached to the support of this fractal set*, which is the price of diamonds as a function of their volume, clearly it is more worthwhile to find large stones than small ones. We must use our knowledge of the distribution of diamonds by bringing in the parameter of their size. Let us suppose that we know the distribution perfectly (otherwise we must take a sample) and let us cover the globe with a grid, attaching to each of its square plots of side ε the monetary value of the diamonds found there. To simplify matters the set of plots of land can be divided into a finite number of batches ($i = 1,...,N$) corresponding to the various slices of value, from the poorest to the richest [to each plot i we attach in this

way its value $\mu(\varepsilon,x_i)$ relative to the total value]. The correspondence of each of these batches to a given slice μ specifies a distribution of diamonds on the earth's surface; we assume that each of these distributions is fractal in the limit when the side ε of the plots tends to zero. The very rare, rich regions will have a fractal dimension close to zero ("dust"), whereas the regions with only a trace of diamonds, albeit uniformly distributed, will have a fractal dimension close to two.

The multifractal character is connected with the heterogeneity of the distribution (see Sec. 1.4.2, and T.A. Witten in Les Houches, 1987). For a homogeneous fractal distribution, the mass in the neighborhood of any point in the distribution is arranged in the same manner. That is to say that inside a sphere of radius R centered on the fractal at x_i, the mass $\mathcal{M}(R)$ fluctuates little about its mean value over all the x_i, $\langle\mathcal{M}(R)\rangle$ whose scaling law is R^D: the distribution $P(\mathcal{M})$ of the masses $\mathcal{M}(R)$ taken at different x_i is narrow, that is, it decreases on either side of the mean value faster than any power. In particular, all the moments vary like $\langle\mathcal{M}(R)^q\rangle \propto \langle\mathcal{M}(R)\rangle^q$, for all q. The fractal distribution is described by the sole exponent D. This is not so for heterogeneous fractals for which there is a broad distribution, $P(\mathcal{M})$, of the masses. Such is the case for the distribution of diamonds on the earth's surface. Knowledge of the behavior of the moments $\langle\mathcal{M}(R)^q\rangle$ tells us about the edges of the distribution, namely the very poor and the very rich regions.

We are going to make these ideas sharper using some simple distributions which will allow us to introduce some mathematical relationships indispensable in the practical use of the concept of multifractility.

The quantities $f(\alpha)$ and $\tau(q)$ (which we are now going to define) will allow us to characterize the distributional heterogeneities of the measures known as *multifractal measures*. As these ideas are not initially obvious, the reader may, if he wishes, turn to the various examples given further on.

1.6.1 Binomial fractal measure

This simple measure is constructed as follows: a segment of length L, on which a uniform measure of density 1/L is distributed, is divided into two parts of equal length: $\ell_0 = \ell_1 = L/2$ to which the weights p_0 and p_1 are given (p_0 to the left and p_1 to the right) (Fig. 1.6.1). This process is iterated ad infinitum. The total measure is preserved if care is taken in choosing

$$p_0 + p_1 = 1.$$

Each element (segment) of the set is labeled by the successive choices (0 left, 1 right) at each iteration. At the n^{th} iteration, each segment is thus indexed by a sequence $[\eta] \equiv [\eta_0, \eta_1, \ldots, \eta_k, \ldots \eta_n]$ where $\eta_k = 0$ or 1, and has length, $d\ell = \varepsilon L = 2^{-n} L$. Its abscissa on the segment E=[0,1] is described simply by the number in base two

$$x = \ell / L = 0.\, \eta_0\eta_1\ldots\eta_n.$$

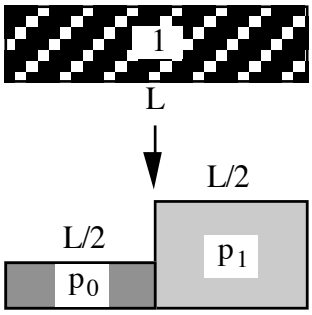

Fig 1.6.1. First iteration of the binomial measure. The measures associated with the areas of the rectangles are shown inside them.

So, at the third iteration, the successive weights $\mu(\varepsilon,x_i)$ are the $p_{[\eta]}$ where

$$
\begin{array}{lll}
[\eta] = [000] & (x_0=0.000) & \rightarrow \; p_{[000]}= p_0{}^3 \\
\quad [001] & (x_1=0.001) & \\
\quad [010] & (x_2=0.010) & \rightarrow \; p_{[001]}= p_{[010]}= p_{[100]}= p_0{}^2 p_1 \\
\quad [100] & (x_3=0.100) & \\
\quad [011] & (x_4=0.011) & \\
\quad [101] & (x_5=0.101) & \rightarrow \; p_{[011]}= p_{[101]}= p_{[110]}= p_0 p_1{}^2 \\
\quad [110] & (x_6=0.110) & \\
\quad [111] & (x_7=0.111) & \rightarrow \; p_{[111]}= p_1{}^3
\end{array}
$$

and so on for each value of n (or of $\varepsilon= 2^{-n}$). For each n, the distribution is normalized to one:

$$\sum_i \mu(\varepsilon, x_i) = \sum_{[\eta]=[00\ldots0]}^{[11\ldots1]} p_{[\eta]} = 1.$$

It can easily be seen that the weight associated with a sequence $[\eta]$ has the general form

$$\mu(\varepsilon, x) \equiv p_{[\eta]} = p_0^{\,n\varphi_0} p_1^{\,n\varphi_1}$$

[$n\varphi_0$ and $n\varphi_1$ being the number of 0's and 1's in $[\eta]$ respectively: $\varphi_0 = k/n$ and $\varphi_1 = (n–k)/n$, $k = 0,\ldots n–1$].

To each value of x is associated a $\varphi_0(x) = 1– \varphi_1(x)$. These weights occur with a frequency

$$N(\varepsilon,x) = \binom{n}{k} = \frac{n!}{(n\varphi_0)!(n\varphi_1)!} \; .$$

Fig. 1.6.2 shows the hierarchy of iterations for n = 4, and the corresponding distribution of weights (more precisely their logarithm). The logarithm of the weight on an interval ε, divided by the logarithm of that interval, is called the *Holder exponent* and is denoted by α ,

$$\alpha = \frac{\log \mu(\varepsilon)}{\log \varepsilon} = -\varphi_0 \log_2 p_0 - \varphi_1 \log_2 p_1$$

It measures the *singular behavior of the measure* in the neighborhood of a point x [via $\varphi_0(x)$ and $\varphi_1(x)$], thus

$$\boxed{\mu(\varepsilon,x) = \varepsilon^{\alpha(x)}}. \qquad (1.6\text{-}1)$$

The values of α are bounded according to the following inequality:

$$0 < \alpha_{min} = -\log_2 p_0 \le \alpha \le \alpha_{max} = -\log_2 p_1 < \infty.$$

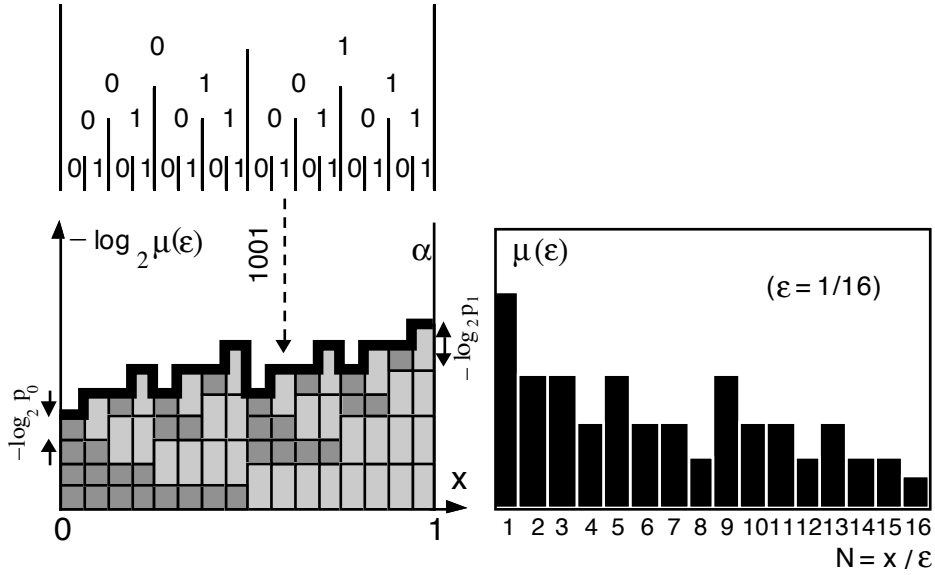

Fig. 1.6.2. (Left) the binary sequences leading to the [η] for n=4. The graph on the right shows the distribution of the measures μ whose logarithm is also proportional (factor –n) to α. Here we have chosen log p_1 = 2 log p_0. We can see the symmetry of the binomial distribution: contrary to the example of the diamonds, the regions of low weight are as rare as those with high weight.

This behavior allows us to partition[8] the set E into subsets having the same α,

$$E = \bigcup_{\alpha} E_\alpha . \qquad (1.6\text{-}2)$$

Let us now take the subsets E_α into closer consideration. We enumerated them above while calculating N(ε). The analog of the Hausdorff dimension for the support of intervals with the same α (function of αand therefore of x) is then written

[8] In our intuitive example about the distribution of diamonds the partition into "batches" is made according to their relative "value;" we see here that these batches may also be designated by their Holder exponents which indicates how the value of a piece of land varies (locally) as a function of its size.

$$\delta(\alpha) = -\frac{\log N(\varepsilon, \alpha)}{\log \varepsilon} \quad . \tag{1.6-3}$$

In the limit of large n (small ε) we have simply

$$\begin{aligned} \delta &= -\log\left[(n\varphi_0)!(n\varphi_1)!/n!\right] / \log \varepsilon \\ &\approx -\varphi_0 \log_2 \varphi_0 - \varphi_1 \log_2 \varphi_1 \quad . \end{aligned}$$

In the binomial case, this fractal dimension is well defined for each set E_α since all the parameters are determined [via $\varphi_0(x)$ and $\varphi_1(x)$].

1.6.2 Multinomial fractal measure

The results just shown for a *binomial measure* easily generalize to *multinomial measures*. By considering b weights p_β ($0 \le \beta \le$ b–1), we can go through an analogous procedure to that of the binomial measure. Each segment of size b^{-n} at iteration n is indexed by a sequence [η] or an abscissa x, written in base b (instead of the 0's and 1's of the previous binomial example). The b-adic intervals are then characterized by the frequencies φ_β of their "digits" in base b. So, the expressions for α and δ generalize to

$$\alpha = -\sum_\beta \varphi_\beta \log_b p_\beta \quad \text{and} \quad \delta = -\sum_\beta \varphi_\beta \log_b \varphi_\beta$$

with the constraints $\sum_\beta \varphi_\beta = 1$ and $\sum_\beta p_\beta = 1$.

In the case of a binomial measure (b = 2), δ is a single valued function of α, since two parameters (φ_0 and φ_1), whose sum is normalized to one, are used. For b > 2, this relationship is no longer single valued (there are b–2 supplementary parameters) and the pairs (α,δ) cover a certain domain. This domain is roughly indicated by a network of curves in Fig. 1.6.3 (for b = 3). The set of [η] (or x expressed in base b) corresponding to the same α is dominated by the term of highest dimension, f = max δ [i.e., by the subset $N(\varepsilon,\alpha)$ whose exponent δ is the greatest]:

$$N(\varepsilon, \alpha)_{\text{dominant}} \propto \varepsilon^{-f(\alpha)} . \tag{1.6-4}$$

This term therefore maximizes

$$-\sum_\beta \varphi_\beta \log_b \varphi_\beta \quad .$$

The variation is thus written, (the $\vartheta\varphi_\beta$ then being independent infinitesimal variables),

$$\vartheta\left(-\sum_\beta \varphi_\beta \log_b \varphi_\beta\right) \equiv 0$$

with the constraints

$$\alpha = -\sum_\beta \varphi_\beta \log_b p_\beta \quad \text{and} \quad 1 = \sum_\beta \varphi_\beta \quad .$$

This is solved in the classical way by introducing Lagrange multipliers q and (r–1), leading to the relation

$$\sum_{\beta} \vartheta\varphi_\beta \, [\, \log_b \varphi_\beta - q \log_b p_\beta - r \,] \equiv 0 \qquad \forall \ \vartheta\varphi_\beta .$$

All the terms inside the brackets vanish. Hence, since the φ_β are normalized to unity (thus determining r):

$$\varphi_\beta = \varphi_\beta(q) = b^r \, p_\beta^q = \frac{p_\beta^q}{\sum_{ß} p_\beta^q}, \qquad -\infty < q < +\infty .$$

The φ's dependence on x now operates via q which picks out the subsets {x}(q) corresponding to δ(α) extreme for fixed α.

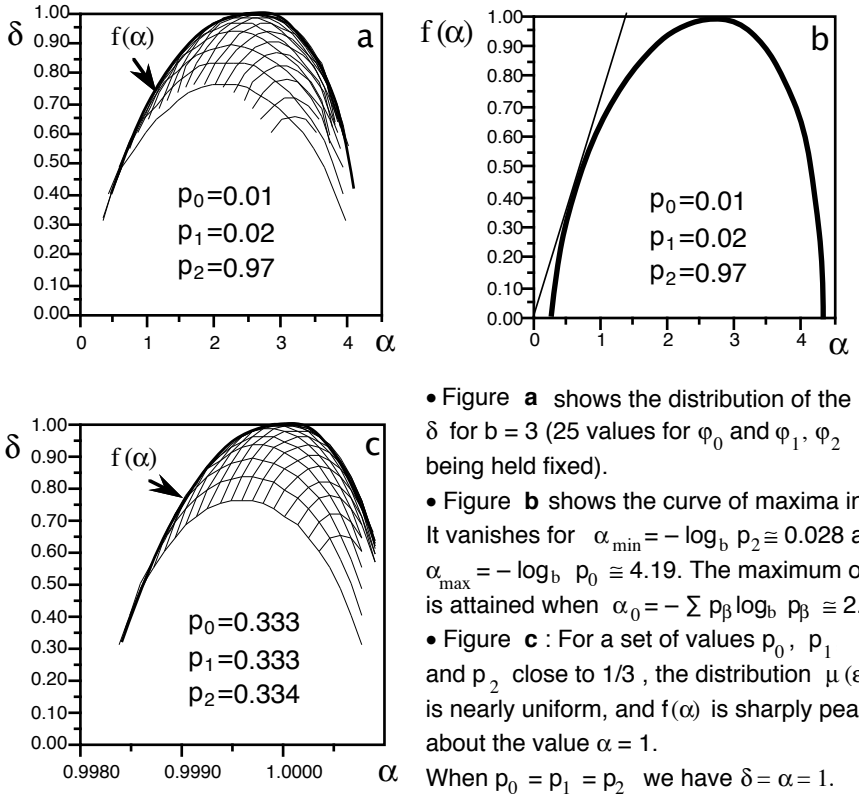

• Figure **a** shows the distribution of the δ for b = 3 (25 values for φ_0 and φ_1, φ_2 being held fixed).

• Figure **b** shows the curve of maxima in f(α) It vanishes for $\alpha_{min} = -\log_b p_2 \cong 0.028$ and $\alpha_{max} = -\log_b p_0 \cong 4.19$. The maximum of f is attained when $\alpha_0 = -\sum p_\beta \log_b p_\beta \cong 2.59$.

• Figure **c** : For a set of values p_0, p_1 and p_2 close to 1/3 , the distribution μ(ε) is nearly uniform, and f(α) is sharply peaked about the value α = 1.

When $p_0 = p_1 = p_2$ we have $\delta = \alpha = 1$.

Fig. 1.6.3. Distribution of the Hausdorff dimensions of subsets E_α .

It is then useful to introduce the quantity

$$\boxed{\tau(q) = \log_b \sum_\beta p_\beta^q}\,. \qquad (1.6\text{-}5a)$$

Very generally $\tau(q)$ enters in the framework of cumulant generating functions. Note that some authors have adopted the opposite sign.

α and $f(\alpha)$ are simply related to $\tau(q)$ by the following relations:

$$\alpha = -\sum_\beta \varphi_\beta \log_b p_\beta = -\frac{\partial}{\partial q} \log_b \sum_\beta p_\beta^q$$

$$\text{and } \max \delta = f(\alpha) = -\left(\sum_ß p_\beta^q [\, q \log_b p_\beta - \log_b \sum_ß p_\beta^q \,] \right) / \sum_ß p_\beta^q$$

which reduce to the remarkable equations

$$\boxed{\alpha = -\frac{\partial \tau(q)}{\partial q} \quad \text{and} \quad f(\alpha) = \tau(q) - q\frac{\partial \tau(q)}{\partial q} = \tau + q\alpha} \qquad (1.6\text{-}5b)$$

with $\alpha = -\sum_\beta \varphi_\beta \log_b p_\beta$, $f(\alpha) = -\sum_\beta \varphi_\beta \log_b \varphi_\beta$,

$$\varphi_\beta = \frac{(p_\beta)^q}{\sum_\beta (p_\beta)^q} \quad \text{and} \quad \tau(q) = \log_b \sum_\beta (p_\beta)^q, \quad -\infty < q < +\infty\,. \qquad (1.6\text{-}5c)$$

These results (constituting the formalism of multifractals) were obtained by Frisch and Parisi (1985) and Halsey *et al.* (1986) using the method of steepest descent. The concept itself already existed in a 1974 paper of B. Mandelbrot. Here we have followed the more straightforward approach of B. Mandelbrot (1988).

It can be seen that the functions $f(\alpha)$ and $\tau(q)$ are Legendre transforms of each other (Fig. 1.6.4). Such transforms are frequently used in thermodynamics when one wishes to change independent variables.

Formally, f may be compared with an entropy, q with the reciprocal of a temperature, α with an energy (conjugate variable of q), and τ with a free Gibbs energy (Lee and Stanley, 1988). The expression for f is indeed that of an entropy or, more precisely, that of a quantity of information, provided that the φ_β are considered to be the probabilities of finding the measures p_β (the relative frequences of the digit β in $x = 0.\eta_0\eta_1\ldots\eta_n$ written in base b). The minimum entropy is obtained when the distribution of the p_β is known exactly, that is, when one of the $\varphi_\beta = 1$ and the others zero (e.g., x = 0.333...33). On the other hand, the maximum disorder or entropy corresponds to all the φ_β being equal [here the φ_β equal 1/b and $f(\alpha) = 1$]. The expression for $\varphi_\beta(q)$ shows that this maximum disorder corresponds either to q = 0, or to the trivial case $p_0 = \ldots p_\beta = \ldots p_{b-1}$ (= 1/b).

Generally speaking, $f(\alpha)$ is a convex, positive curve, increasing from

$f(\alpha_{min}) = 0$ to a maximum $D_0 = \max f(\alpha)$, which is equal to one in the previous example; then $f(\alpha)$ decreases to $f(\alpha_{max}) = 0$. The extreme values of α are given simply by the conditions of minimum entropy (one of the $\varphi_\beta = 1$, all the rest = 0):

$$\alpha_{min} = \min (-\log_b p_\beta), \quad \alpha_{max} = \max (-\log_b p_\beta).$$

Significance of $\tau(q)$

Consider the following measure:

$$M_q(\varepsilon) = \sum_i \mu(\varepsilon, x_i)^q \ . \tag{1.6-6}$$

What does this measure represent?

When $q = 0$, $M_0(\varepsilon)$ represents the volume of support measured in intervals ε, $M_0(\varepsilon) \approx (L/\varepsilon)^{D_0}$, with $D_0 = 1$ here, for the segment [0,1] of length $L = 1$.

When $q = 1$, $M_1(\varepsilon)$ represents the sum over the support of the measures on the ε intervals. As this measure is normalized,

$$M_1(\varepsilon) \equiv \sum_{[\eta]=[00\ldots0]}^{[11\ldots1]} p_{[\eta]} = 1.$$

When $q \to +\infty$, M_q is dominated by the regions of high density μ/ε.

When $q \to -\infty$, M_q is dominated by the regions of low density μ/ε.

Thus, the parameter q allows us to select subsets E_q corresponding to higher or lower densities.

We usually put

$$\boxed{M_q(\varepsilon) = \varepsilon^{(q-1)D_q}}\ ; \tag{1.6-7}$$

an expression which is true for $q = 0$ and $q = 1$. D_q are called *qth order generalized dimensions* [9] (the name is due to Hentschel and Procaccia, 1983), although they are only a dimension when $q = 0$ (D_q can however be defined as a critical dimension when $q > 1$). The advantage of D_q over $\tau(q)$ resides essentially in the fact that the former all reduce to the fractal dimension D when the space is homogeneous, that is,

$$\mu(\varepsilon,x) \ \propto \ \varepsilon^D \quad \forall\ x,$$

for then

$$M_q(\varepsilon) = \sum_{\text{support}} \mu(\varepsilon,x)^q \propto \sum_{\text{support}} \varepsilon^{qD} \propto \varepsilon^{-D}\varepsilon^{qD} \text{ , and hence } \quad D_q = D.$$

Finally, it can be shown that D_q decreases monotonically as q increases.

We shall now show that $(1 - q)D_q = \tau(q)$. From above,

---

[9] Sometimes also called *Renyi dimensions*.

$$M_q(\varepsilon) = \sum_i \varepsilon^{q\,\alpha(x_i)} \quad .$$

Now the number of domains corresponding to the same α is known, it is $N(\varepsilon,\alpha) \propto \varepsilon^{-\delta(\alpha)}$, and hence

$$M_q(\varepsilon) \approx \int_{\alpha_{min}}^{\alpha_{max}} d\alpha\, \varepsilon^{q\,\alpha - \delta(\alpha)}.$$

This integral is dominated by the maxima of $\delta(\alpha)$ with the value of α which minimizes the exponent ($\varepsilon \ll 1$), that is, $\alpha(q)$ such that

$$\frac{\partial}{\partial\alpha}\,[q\,\alpha - \max\,\delta(\alpha)]\,\Big|_{\alpha=\alpha(q)} = 0, \quad \text{where} \quad \max\,\delta(\alpha)\,\Big|_{\alpha=\alpha(q)} \equiv f(\alpha(q))$$

which agrees with the earlier results. By comparison it can be seen that $M_q(\varepsilon) \propto \varepsilon^{q\,\alpha - f}$, hence

$$\boxed{\begin{array}{c} M_q(\varepsilon) \;\propto\; \varepsilon^{-\tau(q)} \\ \text{with} \quad \tau(q) = (1-q)\,D_q = -\lim_{\varepsilon\to 0} \dfrac{1}{\log\varepsilon}\;\log\sum_i \mu(\varepsilon,x_i)^q \end{array}} \quad . \qquad (1.6\text{-}8)$$

(The integral is a discrete sum if the box method is used.)

Form and meaning of D_1

When $q = 1$, the above expression is undetermined. So what is the form and the meaning of D_1, the first order generalized dimension? For this we must calculate

$$D_1 = \lim_{q\to 1}\;\frac{1}{q-1}\;\lim_{\varepsilon\to 0}\;\frac{\log M_q(\varepsilon)}{\log\varepsilon}. \qquad (1.6\text{-}9)$$

Writing $[\mu(\varepsilon,x)^q] = (\mu\,\mu^{q-1}) \cong \mu[1+(q-1)\log\mu]$, so that

$$\log M_q(\varepsilon) = \log\sum_i \mu(\varepsilon,x_i)^q \cong \log\left[1+\sum_i (q-1)\mu(\varepsilon,x_i)\log\mu(\varepsilon,x_i)\right]$$

$$\cong (q-1)\sum_i \mu(\varepsilon,x_i)\log\mu(\varepsilon,x_i)$$

gives

$$\boxed{D_1 = \lim_{\varepsilon\to 0}\;\frac{1}{\log\varepsilon}\sum_i \mu(\varepsilon,x_i)\,\log\mu(\varepsilon,x_i)} \quad . \qquad (1.6\text{-}10)$$

Moreover, we can relate this expression to α and $f(\alpha)$ by differentiating $\tau(q)$. We then find that

$$D_1 = \alpha_{q=1} = f(\alpha_{q=1}) \,. \qquad (1.6\text{-}11)$$

The remarkable property of D_1 comes from the fact that $\sum \mu(\varepsilon)\log\mu(\varepsilon)$ represents the entropy of information of the distribution whose scale behavior D_1 describes. For this reason D_1 is called the *information dimension*. The support set $E_{\alpha(1)}$ contains *almost all the measure* (or mass) of the set E.

In particular, for the multinomial measure on [0,1], we have $\varphi_\beta = p_\beta$ (as q = 1) which means that $D_1 = \Sigma\ p_\beta \log_b p_\beta$. The *information dimension*, as we showed above, reaches a maximum when all the p_β are equal (to 1/b), the information about the distribution then being minimal. On the other hand, D_1 is zero when all the p_β are zero except one, p_β. The information is then complete since the whole measure is on one abscissa point x = 0. βββ…

To finish, let us now calculate the mass exponent of the measure distribution $\mu(\varepsilon,x)^q$ using the η-dimensional Hausdorff measure (see Sec. 1.3). It is found as the sum of volume elements ε^η, weighted by their associated measure μ^q, that is,

$$m_\eta(E,\mu^q) = \lim_{\varepsilon\to 0} \sum_i \mu(\varepsilon, x_i)^q \varepsilon^\eta = \lim_{\varepsilon\to 0} M_q(\varepsilon)\, \varepsilon^\eta .$$

From what we saw earlier we find that

$$m_\eta(E,\mu^q) = \begin{cases} \to 0 & \text{if } \eta > \tau(q) \\ \to \infty & \text{if } \eta < \tau(q) \end{cases} .$$

τ(q) is therefore the mass exponent of the distribution μ^q. This result is trivial here because there is only one dilation scale (a factor 1/2 for each segment at each iteration). When *nonuniform fractals* are considered, several dilation scales are present and this formulation proves to be the most direct method of calculating τ(q) and the other multifractal characteristics.

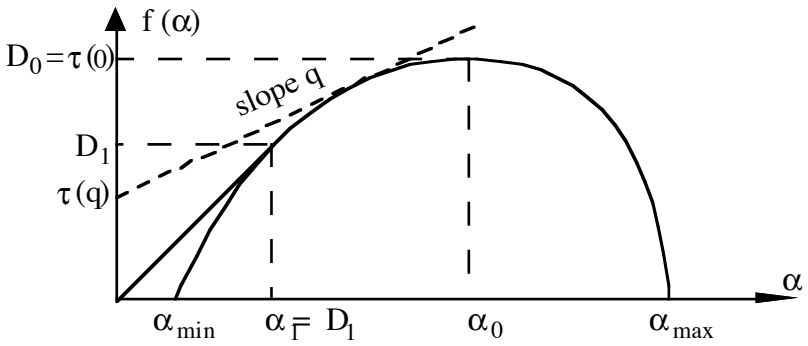

Fig. 1.6.4. The Legendre transform allows one to pass from the equation f = f(α) of a plane curve to the equation τ=τ(q) of the same curve by eliminating α between q = df/dα and τ = f – qα.

Significance of the maximum of f(α)

The maximum of f(α) corresponds to ∂f/∂α≡ q = 0, and consequently to all the φ_β equaling 1/b,

$$M_0(\varepsilon) = (L/\varepsilon)^{D_0} \quad \text{with} \quad \tau(0) = \max f(\alpha) = f(\alpha(0)) = D_0 .$$

$D_0 = 1$ in the multinomial example.

The maximum of f(α) therefore corresponds to a uniform measure on the

support. Its value is thus the dimension (fractal or otherwise) of the support. Here, it is that of a segment [0, L] and therefore equals one.

Everything that has been developed for the multinomial case will contribute to understanding the general case of a distribution of measures over a fractal support. We shall approach this subject by explaining in detail two important measures for physics, the multifractal measure of a distribution of points, mass or current (developed turbulence, strange attractors, distributions of galaxies or flux of matter in a porous rock, resistors networks), and the harmonic multifractal measure (growth phenomena, DLA, etc.). Remaining within the general framework, some structures which are fractal on several scales, with multifractal characteristics which may be fully calculated, will be considered.

1.6.3 Two-scale Cantor sets

The Cantor sets mentioned in Sec. 1.4.1 with their uniform measures are not multifractal; in fact their curves $f(\alpha)$ reduce to a point [$\alpha = f(\alpha) = D$]. They are pure fractals. To generate a multifractal structure with a uniform measure at least two dilation scales must be used.

Let us examine one of these structures by treating the general case: two measure scales, two dilation scales. The following structure (Cantor bars) generalizes the binomial measure studied above. An initial segment of length L and unit measure (mass) is divided into two parts: ℓ_0 and ℓ_1 to which we associate the measures p_0 and p_1 ($p_0 + p_1 = 1$). The first three steps of the construction are shown in Fig. 1.6.5.

Determination of $\tau(q)$

$\tau(q)$ will be determined by calculating the η-dimensional Hausdorff measure. In practice the result is completely analogous to that giving the fractal dimension calculated from Eq. 1.4-2. We therefore calculate

$$m_\eta(q,N) = \sum_{i=0}^{N-1} \mu_i^q \ell_i^\eta = \underset{\varepsilon \to 0}{\rightarrow} \begin{cases} \rightarrow 0 & \text{if } \eta > \tau(q) \\ \rightarrow \infty & \text{if } \eta < \tau(q) \end{cases} \qquad \text{where } \varepsilon = \max(\ell_i) .$$

In the present case, i = [0, N–1] designates the i th element out of $N = 2^n$, (n being the number of iterations). It takes the place of x in the binomial measure. The measure and the size of the i th element are, respectively,

$$\mu_i = p_0^k p_1^{n-k} \quad \text{and} \quad \ell_i = \ell_0^k \ell_1^{n-k}$$

and its degeneracy is the number of ways of choosing k objects out of n without regard to order of choice. Thus,

$$m_\eta(q,N) = \sum_{k=0}^{n} \binom{n}{k} (p_0^k p_1^{n-k})^q (\ell_0^k \ell_1^{n-k})^\eta = \left(p_0^q \ell_0^\eta + p_1^q \ell_1^\eta\right)^n$$

$$m_\eta (q,N) \underset{n\to\infty}{\to} \begin{cases} \to 0 & \text{if } p_0^q \ell_0^\eta + p_1^q \ell_1^\eta < 1 \quad (\eta > \tau(q)) \\ \to \infty & \text{if } p_0^q \ell_0^\eta + p_1^q \ell_1^\eta > 1 \quad (\eta < \tau(q)) \end{cases}$$

and $\tau(q)$ is determined by the equation [analogous to that of Sec.1.4.1, Eq. (1.4-2)]

$$p_0^q \ell_0^{\tau(q)} + p_1^q \ell_1^{\tau(q)} = 1$$

Knowing $\tau(q)$ we can also calculate D_q, α, and $f(\alpha)$. For a generalization to several scales see Hentschel and Procaccia (1983).

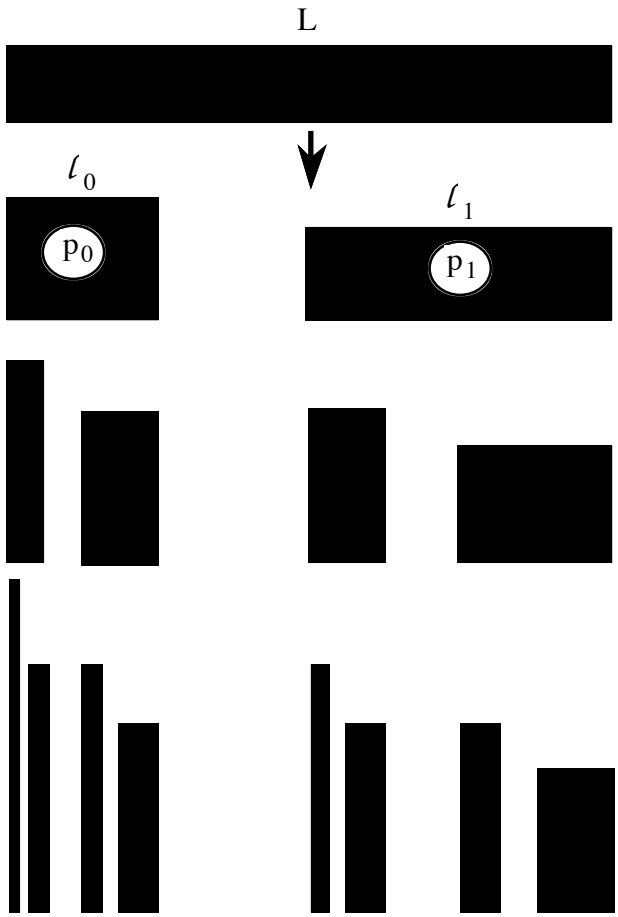

Fig. 1.6.5. The three first iterations of the Cantor set weighted by dilation scales $\ell_0 = L/4$ and $\ell_1 = L/2$ and weights $p_0 = 0.4$, $p_1 = 0.6$.

1.6.4 Multifractal measure on a set of points

Any statistical description of a set of points uses the notion of correlation, more or less directly. Indeed, these correlations represent deviations from a uniform distribution of points (i.e., translational invariance).

One way of determining these correlations is by calculating the moments of the distribution of points. For this the box-counting method may be used (see Sec. 1.3.3) and a measure defined in each box of side ε centered at x.

The number of points inside a box is $\mathcal{N}(\varepsilon,x)$, so that the probability of finding a point is $\mathcal{N}(\varepsilon,x)/\mathcal{N}$, $\mathcal{N}$ being the number of points in the set.

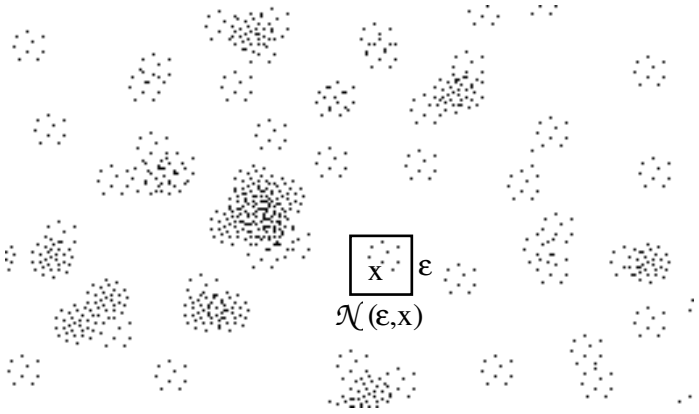

Fig. 1.6.6. Multifractal measure of a cloud of points. Use of the box-counting method.

$$\mu(\varepsilon,x) = \mathcal{N}(\varepsilon,x)/\mathcal{N}$$

will therefore represent our measure. Its $(q-1)$th order moment may be calculated by summing over the boxes:

$$\langle \mu(\varepsilon)^{q-1} \rangle = \sum_{i \in \text{boxes}} \mu(\varepsilon,x_i)^q = M_q(\varepsilon) \ .$$

If the structure is multifractal, from above, μ and M display the power laws,

$$\mu(\varepsilon,x) \propto \varepsilon^{\alpha(x)} \quad \text{and} \quad M_q(\varepsilon) \propto \varepsilon^{-\tau(q)} = \varepsilon^{(q-1)D_q}$$

the exponent $\alpha = \alpha(q)$ is the same for all $x \in E_{\alpha(q)}$.

Having found $\tau(q)$ via

$$\tau(q) = -\frac{\log M_q(\varepsilon)}{\log \varepsilon}$$

$\alpha(q)$ and $f(\alpha)$ may then be calculated, using the relations obtained for the multinomial measure

$$\alpha = -\frac{\partial \tau(q)}{\partial q} \quad \text{and} \quad f(\alpha) = \tau + q\alpha,$$

since their derivation is general. What is new here, in relation to the multinomial measure, is that the support (set of points) may itself be fractal. This description may be used to characterize the strange attractors obtained in chaotic phenomena. We shall give some examples of this in Sec. 2.3.

For a more complete (but also more difficult) justification of the above

formalism, Collet et al. (1987), Bohr and Rand (1987), Rand (1989), and Ruelle (1982, 1989) may be consulted.